Journal of Materials Chemistry C

Accepted Manuscript

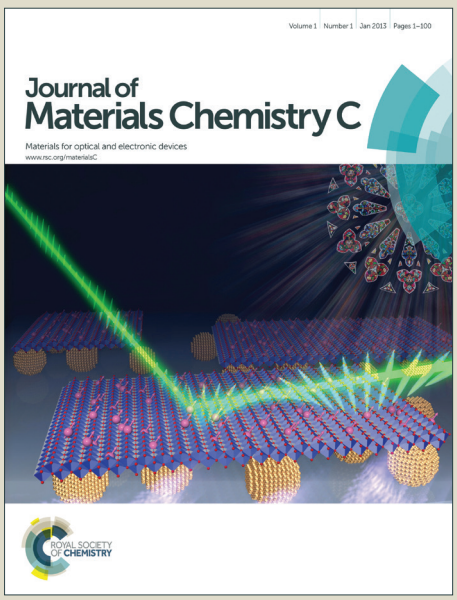

ROYAL SOCIETY OF CHEMISTRY

www.rsc.org/materialsC

Journal of Materials Chemistry C RSCPublishing

COMMUNICATION

Crystalline Structure-Tunable, Surface Oxidation-Suppressed Ni Nanoparticles: Printable Magnetic Colloidal Fluids for Flexible Electronics

Cite this: DOI: 10.1039/xoxxoooooox

Received ooth January 2012,
Accepted ooth January 2012

DOI: 10.1039/xoxxoooooox

www.rsc.org/nanoscale

Yejin Jo,[a] Sang-Jin Oh,[a,b] Sun Sook Lee,[a] Yeong-Hui Seo,[a] Beyong-Hwan Ryu,[a] Dae Ho Yoon,[b] Youngmin Choi,[a,*] Sunho Jeong[a,*]

In this study, we suggest the chemical methodology that allows for the facile controllability of phase transformation between face-centered cubic and hexagonal close-packed structure for Ni nanoparticles with a 0.4 - 2 nm thick shallow surface oxide layer, resulting in a maximum saturation magnetization of 33.2 emu/g. As a first proof-of-concept of the potential for flexible, printed magnetic devices on cost-effective polyethylene terephthalate (PET) and paper substrates, it is demonstrated that the resulting Ni nanoparticles, prepared in the form of magnetic fluids, are transformed into bulk-like patterned Ni architectures by an air-brush printing and an instant photonic annealing in a timescale of 10^{-3}sec, exhibiting the highly flexible properties under harsh conditions of 10,000 times repeated bending tests.

Introduction

In recent decades, chemically synthesized metallic nanoparticles have attracted much attention in various research fields by virtue of the size-dependent modulation of electronic, optical, catalytic, and magnetic properties. In particular, Au, Ag, Cu nanoparticles have been widely studied in the field of plasmonics-involved optoelectronics,[1,2] flexible electronic devices,[3-5] and next generation stretchable electronics,[6,7] together with a strategic investigation of unconventional printing techniques. In addition to those highly conductive metallic components, nanostructured Ni particles could open the way to other possible applications ranging from magnetically modulated devices to bio-devices, owing to their characteristic magnetic properties.[8-11] However, to date, a device-applicable, printable Ni nanoparticle fluid based on a wet patterning process for flexible applications has been not suggested, unlike the cases of non-magnetized, conductive metallic Au, Ag, Cu nanoparticles.

From the viewpoint of crystalline structure evolution, the facile adjustment of crystalline phases is not easily achievable in chemically derived Ni nanoparticles. On a thermodynamic basis, the nickel exists as a face centered-cubic (FCC) crystalline structure with ferromagnetic properties under ambient conditions. Even with the introduction of elevated temperature environments, achieving a crystalline phase evolution into a metastable hexagonal close-packed (HCP) phase is highly demanding. There have been a limited number of reports on the chemical path that can lead to the possibility of HCP Ni phase formation.[12-15] However, interestingly, there has been no analytical study on the suppression of surface oxidation-related magnetic properties in chemically synthesized Ni nanoparticles, even with the classical knowledge on the adverse impact of surface oxides on magnetic properties.[16-18]

In previous reports, the crystalline phase has been adjusted mainly by varying the reaction temperature in a thermodynamically-controlled way,[12-14] which inevitably affects the susceptibility of oxygen molecules into nickel nuclei, even through surface capping layers, resulting in the uncontrollable surface oxidation. Compared with easily reductive Au, Ag nanoparticles, the control of surface oxide formation in Cu, Ni, Co nanoparticles is particularly challenging when using wet-chemical synthetic pathways. Thus, it is necessary to utilize a chemical route which is capable of tailoring both the chemical structure and the surface oxide formation, in order to adjust the magnetic properties on demand. To date, most researches on Ni nanoparticle synthesis have been focused on modulating the size-dependent superparamagnetic property in monodisperse particle systems[19,20] and tailoring the morphological properties.[21,22]

In this study, we report a wet-chemical methodology for adjusting the chemical/physical properties of Ni nanoparticles, in conjunction with a comparative analysis on their chemical structure, magnetic property, and surface oxide layer formation. For this purpose, a chemical route for synthesizing Ni nanoparticles is demonstrated based on the combinatorial chemical interaction of oleyamine, oleic acid, and phenyhydrazine. In addition, in order to illustrate potentials as a printable magnetic nano-colloidal fluid for flexible applications, the Ni nanoparticle-suspending solution is

Table 1. The compositions of each reactant in batches for synthesizing the Ni nanoparticles

Sample #	$Ni(acac)_2$	Oleic acid		phenylhydrazine		oleylamine	Temp.
1		0	0	0	0		
2		2.2 g	0.1M	0	0		
3		6.6 g	0.3M	0	0		
4	5.05 g	0	0	116.4 g	6.2 M	71.8 g	240 °C
5		0	0	87.3 g	5.5 M		
6		0	0	58.2 g	4.5 M		
7		0	0	29.1 g	2.9 M		

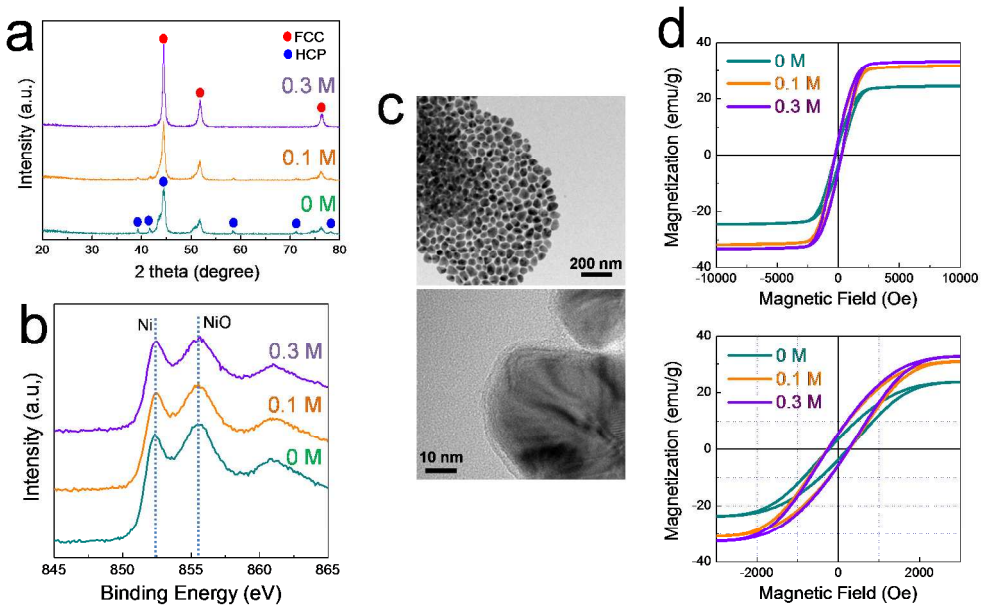

Figure 1. (a) X-ray diffraction results and (b) X-ray photoelectron spectroscopy spectra of Ni $2p_{3/2}$ for Ni nanoparticles synthesized with different concentrations of oleic acid, 0 M (sample #1), 0.1 M (sample #2), and 0.3 M (sample #3), without the presence of phenylhydrazine. (c) High resolution transmission electron microscopy images of Ni nanoparticles (sample #3) and (d) field-dependent magnetization of Ni nanoparticles (samples #1, 2, 3).

transformed into patterned Ni bulk structures on flexible polyimide (PI), polyethylene terephthalate (PET) and paper substrates, through a facile air-brush printing technique combined with a flash photonic annealing process in air.

Results and Discussion

The Ni nanoparticles were synthesized from an organometallic precursor, nickel acetylacetonate, in oleylamine as a solvent at 240 °C under Ar atmosphere. The oleylamine, which was incorporated as both the solvent medium and the capping molecule, also acts as a reducing agent for forming the nickel nuclei at an elevated temperature. The role as a reducing agent of oleylamine has been commonly reported in the synthesis of chalcogende nanoparticles.[23,24] The synthesis conditions are summarized in Table 1. As shown in Figure 1a and Figure S1, the crystalline structure of the resulting Ni nanoparticles appeared to be a mixture of FCC and HCP phases, which results from the chemical role of the amine group in oleylamine adsorbed on the Ni nanoparticle surface.[12,13] When the oleic acid was incorporated as another capping molecule, the HCP phase evolution was effectively suppressed by increasing the amount of oleic acid, from 0 to 0.3 M. This was due to the restricted interaction of oleylamine, caused by the spatial presence of oleic acid around the surface of the nickel nuclei. To obtain accurate chemical structural information for each Ni nanoparticle, an X-ray photoelectron spectroscopy (XPS)-based analysis was carried out (Figure 1b). The peaks at 852.3 and 855.3 eV are attributed to Ni and NiO, respectively. It was observed that even with the chemically induced vigorous phase evolution, the XPS spectra were almost identical, indicative of the well-controlled surface oxidation behavior. It should be noted that the XPS analysis is limited to the outer surface of the measured samples; thus, the relative ratio obtained from the XPS spectra does not imply the absolute volumetric fraction of surface oxide. As seen in HRTEM images, used for observing the surface oxide thickness (Figure 1c), individually isolated Ni nanoparticles with a particle size of ~50 nm were coated with a 2 nm-thick shallow layer; thus, it is

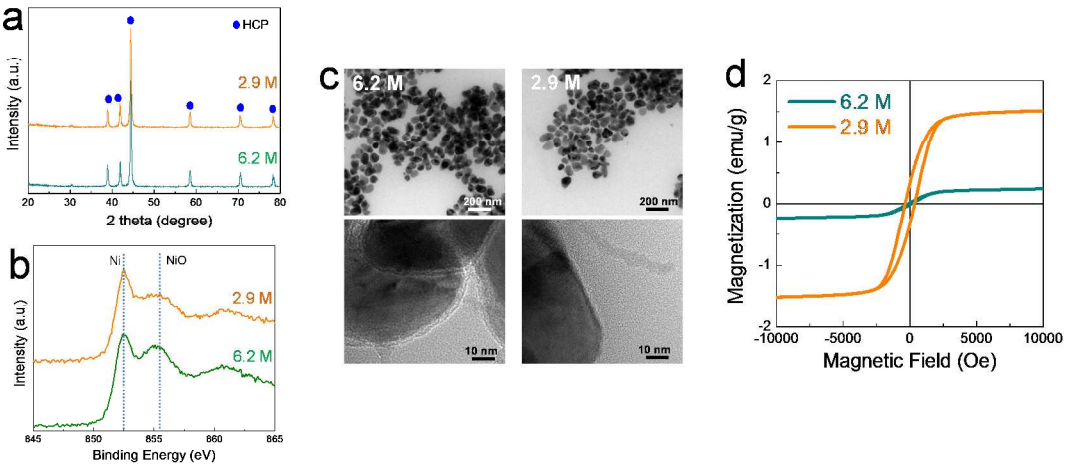

Figure 2. (a) X-ray diffraction results and (b) X-ray photoelectron spectroscopy spectra of Ni $2p_{3/2}$ for Ni nanoparticles synthesized with different concentrations of phenylhydrazine, 6.2 M (sample #4), and 2.9 M (sample #7), without the presence of oleic acid. (c) High resolution transmission electron microscopy images of Ni nanoparticles (samples #4, 7) and (d) field-dependent magnetization of Ni nanoparticles (samples #4, 7).

believed that the shell layer is composed of thin oxide phase along with organic capping molecules. Note that the resulting Ni nanoparticles did not suffer from interparticular aggregation under highly concentrated synthetic conditions (Ni precursor concentration of 0.3 M), which indicates the chemical synthesis pathways were well tailored for achieving both vigorous chemical growth, and effective surface capping by oleylamine with an elongated linear chain structure. The Ni nanoparticles were readily dispersed with a concentration of 20 - 50 wt% in non-coordinating solvents after a slight agitation. On the basis of an XPS-based chemical structural analysis, it can be deduced that the magnetic property of the phase-controlled nanoparticles is solely determined by the crystalline phase, excluding the relevant influence of surface oxidation. In fact, the saturation magnetization and remanent magnetization varied from 33.2 to 24.5 emu/g and from 8.5 to 5.6 emu/g, respectively, upon the evolution of the HCP phase in exchange for the ferromagnetic FCC phase. The magnetic properties of FCC Ni nanoparticles, synthesized in this study, are comparable to phase pure FCC Ni nanoparticles derived from other chemical methodologies.[12,25]

To further manifest the phase evolution toward the HCP phase, phenylhydrazine was introduced as another additive to enhance the N-Ni chemical interaction, in the absence of oleic acid. In previous studies, both alkylamines and ethylenediamine were incoporated for tailoring the N-Ni chemical interaction.[12,13,26] Phenylhydrazine is a well-known reducing agent in common organometallic precursor-based solvothermal reactions.[27,28] However, in our synthetic conditions, the abundant oleylamine acts as a primary reducing agent over phenylhydrazine; this is supported by the fact that similar morphological properties, size and shape, were obtained for all of Ni nanoparticles synthesized with the different additional amount of phenylhydrazine. As shown in Figures 2a and S2, upon the addition of phenylhydrazine with a range of 2.9 to 6.2 M, the FCC phase was clearly extinguished, with the formation of pure HCP Ni nanoparticles. This implies that an instant phase change is effectively achievable through the chemically modified synthesis pathway, and is not related to a previously-reported temperature dependent phase modulation. Furthermore, the competitive interaction of phenylhydrazine and oleylamine toward Ni nuclei enhanced the control over the formation of surface oxide. Under a compositional range of phenylhydrazine from 4.5 to 6.2 M, the chemical structures, obtained from XPS analysis, did not vary (Figures 2b and S3); but, with the addition of 2.9 M phenylhydrazine, the surface oxide fraction was drastically diminished (Figure 2b). This suppression of surface oxidation was also confirmed from HRTEM images, as shown in Figure 2c. The thickness of the amorphous surface layer was reduced from 1.6 to 0.4 nm by decreasing the phenylhydrazine concentration from 6.2 to 2.9 M. The long chain-structure capping molecules have been known to create a favorable result by effectively surrounding the surface of even easily oxidized metallic nuclei.[29] Thus, it can be suggested that the synthesis method based on the combinatorial interaction of oleylamine, as both the primary reducing agent and the surface passivation agent, and phenylhydrazine, as a crystalline phase modulator, provides a chemical pathway for facilitating the control of the surface oxidation and crystalline phase. The critical impact of surface oxide on the magnetic property of Ni nanoparticles is clearly shown in Figure 2d and S4. With the presence of a slightly thicker surface oxide, the HCP Ni nanoparticles were almost magnetically inactive. The saturation magnetization and remanent magnetization were significantly degraded from 1.5 to 0.2 emu/g and from 0.5 to 0.03 emu/g, respectively, depending on the degree of surface oxidation.

The highly magnetized Ni nanoparticles were formulated as a printable, stable liquid phase by dispersing in non-coordinating solvent, toluene. As shown in Figure 3a, the prepared FCC Ni nano-colloid suspension, with a solid loading of 20 wt% in toluene, was stable without the time-dependent formation of precipitates, and the magnetic properties of the Ni nanoparticles were well maintained even in a liquid phase. Then, by diluting with toluene, a Ni nanoparticle suspension of 0.7 wt%, suitable for air-brush printing, was prepared. For practical application to electronic/magnetic devices, the Ni nanoparticles should be transformed into a bulk phase after the structure forming processes, except for applications which are based on the particle size-dependent superparamagnetism. In particular, in the case of flexible/stretchable devices, the individual nanoparticle assemblies would not be robust against mechanical deformation, without additional overcoat-layers. In

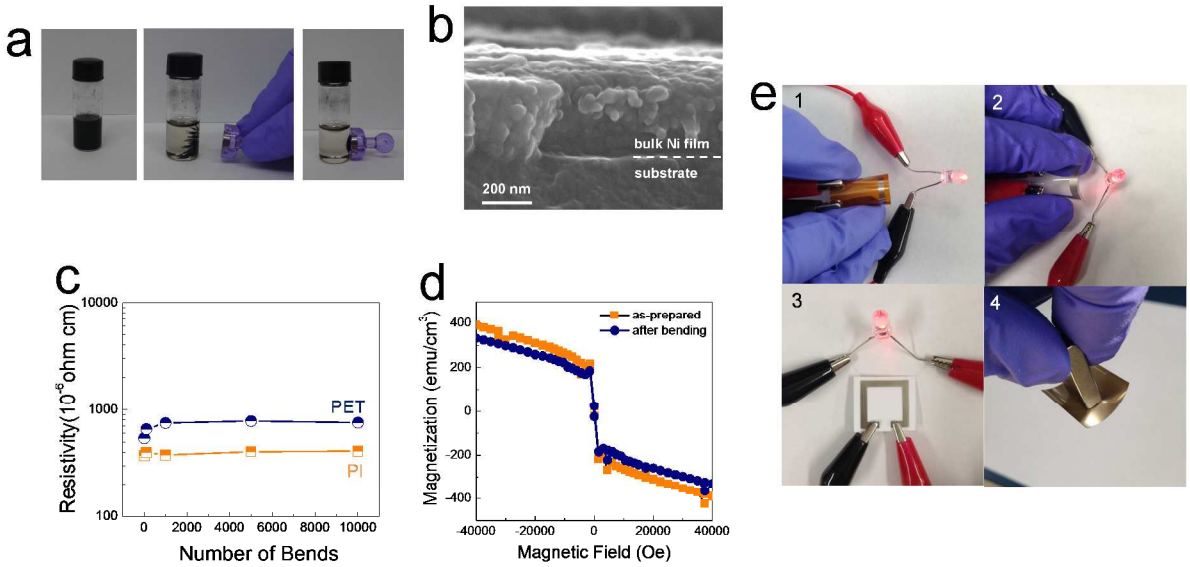

Figure 3. (a) Photographs of printable Ni nanoparticle suspensions; as the Ni nanoparticle suspension moves closer to a magnet, the Ni nanoparticles dispersed in toluene becomes attracted to a magnet, (b) SEM image of printed Ni film after photonic annealing at 2.5 kV for 1 msec. (c) Resistivity variation of photo-annealed Ni bulk film under repeated bending cycles up to 10,000. (d) Field-dependent magnetization of photo-annealed Ni bulk film before/after 10,000 cycle bending test. (e) Photographs demonstrating the bulk-like properties of photo-annealed, air brush-printed Ni layers on PI (1,4), PET (2), and paper substrates (3).

general practice, particulate layers are structurally transformed through a thermally triggered densification reaction. However, the Ni nanoparticles cannot be sintered below 400°C, the temperature limit at which the plastic substrates, including engineered polyimide films, can stably survive. The Ag nanoparticles that can be sintered around 100-200°C have been demonstrated in various flexible/stretchable devices;[6,28,30,31] but, easily oxidizable metal nanoparticles require annealing processes at much higher temperatures, owing to the presence of the inherent surface oxide layer that hinders effective mass transport.[32] Moreover, Ni has a higher melting point, compared with conventionally reported Au, Ag, Cu nanoparticles (melting points of bulk Ag, Ag, Cu and Ni are 1054, 951, 1074, and 1443 °C, respectively),[33] which makes it difficult to activate the inter-particular diffusion for a sintering process at low temperatures.

To facilitate the fabrication of Ni nanoparticle-derived structures that are compatible even with thermally vulnerable PET and paper substrates, we carried out a photonic annealing process in air using the irradiation of a UV-visible light flash ranging from 240 to 800 nm and lasting ~10^{-3}sec, without damaging the underlying substrates. The Ni nanoparticles (sample #3) with a pure FCC phase were used for deriving the highly magnetized flexible structures. It was revealed that our Ni nanoparticles absorb the most photons at wavelengths of 300-850 nm (Figure S5), which implies that UV-visible light can be an appropriate energy source for triggering the inter-particular mass transport. For quantitative analysis of the structural transformation, we measured the resistivity of photo-annealed Ni particulate films. The evolution in resistivity is determined predominantly by both bulk oxidation behavior and degree of densification. During the photonic annealing process, no further oxidation took place, and the shallow oxide phase underwent the photo-chemical reduction (Figure S6); thus, the in-situ analysis of resistivities can be used as a representative way of investigating the degree of structural transformation.

The photon energy dose as a function of voltage and time, are summarized in Figure S7. As shown in Figure S8, for printed Ni features, whereas the Ni particulate film was highly resistive when processed with an insufficient energy dose, the resistivities of 309-540 μΩ·cm were measured with an energy dose between 1.3 and 2.0 J/cm^2 below 2.5 kV. The resistivity of nanoparticle-derived Ag conductive film was, in general, 3-5 times higher than that of corresponding pure bulk one, owing to the presence of micro- or nano-pores and impurities,[28,31,34] and the resistivity varied significantly for the Cu nanoparticle-based film, depending on the volume fraction of insulating surface oxide.[32] Thus, taking the resistivity, 6.8 μΩ·cm, of pure bulk Ni into consideration, it is believed that the resistivity of the photo-annealed Ni film is indicative of the formation of sufficiently densified bulk-like Ni structures. As seen in Figure 3b, after the instantaneous photonic annealing under an energy dose of 1.3 J/cm^2 (2.5 kV, 1 msec), the particulate film was transformed completely into a bulk dense film structure. In the case of a PET substrate, when Ni nanoparticle layers were photo-annealed at 2.0 KV for 1.5- 2.0 msec, a resistivity of 543 μΩ·cm was obtained, similar to the case using polyimide substrates. The obtained Ni structures on both PI and PET substrates were highly durable against repeated bending, as established by a bending test of 10,000 times (Figure 3c). The electrical properties did not significantly vary during a prolonged bending condition, regardless of the kind of substrate. The slight increase in the beginning of the bending test was attributable to the release of internal stress accumulated inside films during the instant structural transformation.

According to the field-dependent magnetization results (Figure 3d), obtained by SQUID analysis for photo-annealed Ni films, the magnetic properties were also well preserved, with a saturation magnetization of 332 emu/cm^3 after completing the bending test during 10,000 cycles. The saturation magnetization of unstressed photo-annealed Ni films was measured to be 391 emu/cm^3. This excellent bending behavior is characteristic of

the bulk property of thin metallic Ni films adhered well to polymeric substrates (Figure S9), and not of individually separated-nanoparticle structures. To date, in a limited number of previous studies, a PET substrate-compatible metal nanoparticle has been reported only for the silver that does not undergo undesirable surface oxidation.[35,36] In addition, the level of bending durability demonstrated during the repeated bending test of 10,000 times has been not widely achieved in other printed patterned structures. These results suggest that the proposed flash photonic annealing methodology could represent a new effective pathway for fabricating electrically and/or magnetically activated flexible Ni structures, when combined with well-tailored functional Ni nanoparticles. As shown in Figure 3e, after the photonic annealing under conditions suitable to each substrate, the air-brush printed Ni patterns were active electrically or magnetically, showing flexible, bulk-structural properties even on cost-effective PET and paper substrates.

Conclusion

In summary, we demonstrated the chemical synthesis methodology, based on Ni acetylacetonate, oleylamine, oleic acid, and phenylhydrazine, that facilitates the adjustable phase transformation from FCC to HCP by the competitive interaction of incorporated chemical moieties, with the suppression of surface oxide formation. It was revealed that the saturation magnetization of Ni nanoparticles was tuned from 33.2 to 0.2 emu/g depending on the relative fraction of crystalline structures, without the involvement of an unpredictable evolution of surface oxide layer. The wet-phase printability of magnetic Ni fluids prepared in the form of a colloidal suspension was, for the first time, demonstrated with air-brush printing techniques, along with their structural transformation into bulk phases on cost-effective PET and paper substrates through the instant photonic annealing for 1 msec, showing the stable flexibility even after 10,000 cycle bending tests.

Experimental

Ni(II) acetylacetonate ($Ni(C_5H_7O_2)_2$, 95%), oleylamine ($C_{18}H_{35}NH_2$, 99%), oleic acid ($C_{18}H_{34}O_2$, 90%), phenylhydrazine ($C_6H_5NHNH_2$, 97%), and toluene ($C_6H_5CH_3$, anhydrous, 99.8%) were purchased from Aldrich, and used as received without further purification. Ni nanoparticles were synthesized via chemical reduction of Ni ions in octylamine under inert atmosphere, and the details on synthesis conditions were summarized in Table 1. Ni acetylacetonate and oleic acid were added into a three-neck round-bottomed flask containing octylamine. The flask was fitted with a reflux condenser and a mechanical stirrer. The solution was purged with nitrogen for 60 min. Then, the solution was heated to 240 ^oC, and if necessary, the hydrazine was injected at 240 ^oC with an injection rate of 2 ml/min. The reaction was continued for 60 min. After completion of the synthesis reaction, the synthesized Ni nanoparticles were separated by centrifugation in air and washed with toluene and chloroform. The synthesized Ni nanoparticles were kept in air without additional surface-passivation procedures.

For preparation of the printable Ni nanoparticle suspension, the obtained Ni nanoparticles, with a solid loading of 20 wt%, were dispersed in toluene with the addition of dispersant. The prepared suspensions were subjected to ball milling for 1 hr, and then diluted down to 0.7 wt% by adding excessive toluene to make a fluid suitable for the air brush-printing method. For air-brush printing, the preparation of suspension with an appropriate solid loading is important to form uniform films without the involvement of nozzle clogging. With a higher solid loading, the morphologically-uneven films were obtained. For the case of ink with a lower solid loading, it took long to deposit 300 nm-thick films. A commercially available pneumatic spray nozzle (Iwata, HP-CP) was used, and the Ni nanoparticle suspension was printed onto PI (Kapton film 300HN, Teijin DuPont Films, 75 μm), PET (Tetoron KEL86W, Teijin DuPont Films, 125 μm) and photo paper (Epson premium photo paper semi-gloss, basis weight of 251 g/m^2) substrate in air using a metallic shadow mask. During the printing process, the distance between substrate and nozzle was 15 cm, and the substrate temperature was maintained at 100 ^oC. Photonic annealing was accomplished in air using a xenon flash lamp system (Sinteron 2010, Xenon Corp.) which was equipped with the B type lamp with a broadband spectrum of 240 to 800 nm. The air cooled xenon linear flash lamp, located 2 inches away from the substrate stage, delivered the optical energy of from 0.39 to 2.44 J/cm^2, as a function of an electrical voltage and a duration time to generate the electrical pulse energies. The optical energies of the flash lamp irradiation were measured by a radiometer (ITL1700, International light technologies) with a detector (SED033, 200-1100 nm, International light technologies).

The size and shape of the synthesized Ni nanoparticles, and the microstructures of the Ni layers were observed by a transmission electron microscope (TEM, JEM-4010, JEOL) and a scanning electron microscope (SEM, JSM-6700, JEOL). The crystal structure of Ni nanoparticles was analysed using an X-ray diffractometer (XRD, D/MAX-2200V, Rigaku) and the chemical structural analysis of Ni nanoparticles was performed with X-ray photoelectron spectroscopy (XPS, K-Alpha, Thermo Fisher Scientific). For XPS spectra, we did not carry out the base line correction in order to avoid the distortion of obtained spectrum data. The absorption spectrum for the Ni nanoparticle film was measured using an UV-Vis spectroscopy (UV-2501PC, 200-1100 nm, Shimadzu). The resistivity of Ni layers was analysed by a four point probe (FPP-HS8, Dasol Eng.) and magnetic hysteresis curves were measured using a superconducting quantum interference device (SQUID, MPMS3, Qantum Design) at 300 K. The flexibility test was carried out with a bending radius of 7 mm using a bending machine (PMC-1HS, Autonics).

Acknowledgements

This research has been supported by the Korea Research Institute of Chemical Technology (KRICT) core project funded by the Ministry of Science, ICT and Future Planning, and partially supported by the R&D Convergence Program of NST (National Research Council of Science & Technology) of Republic of Korea.

Notes and references

[a] Division of Advanced Materials, Korea Research Institute of Chemical Technology (KRICT), Daejeon 305-600, Republic of Korea.
E-mail: youngmin@krict.re.kr; sjeong@krict.re.kr
[b] Department of Advanced Materials Engineering, Sungkyunkwan University, Suwon 440-746, Republic of Korea.

Electronic Supplementary Information (ESI) available: XPS, and field-dependent magnetization for Ni nanoparticles (sample #5, #6), UV-visible spectrum for Ni nanoparticle film, XPS spectrum for photo-annealed Ni film, the dose and intensity of photon energy irradiated from a flash lamp, the resistivity evolution depending on processing parameters

in a photonic annealing, and adhesion test results for photo-annealed Ni films. See DOI: 10.1039/c000000x/

1 H. Choi, S.-J. Ko, Y. Choi, P. Joo, T. Kim, B. R. Lee, J.-W. Jung, H. J. Choi, M. Cha, J.-R. Jeong, I.-W. Hwang, M. H. Song, B.-S. Kim, J. Y. Kim, *Nat. Photonics,* 2013, **7**, 732-738.

2 H. A. Atwater, A. Polman, *Nat. Mater.,* 2010, **9**, 205-213.

3 A. Russo, B. Y. Ahn, J. J. Adams, E. B. Duoss, J. T. Bernhard, J. A. Lewis, *Adv. Mater.,* 2011, **23**, 3426-3430.

4 S. Jeong, H. C. Song, W. W. Lee, H. J. Suk, S. S. Lee, T. Ahn, J.-W. Ka, Y. Choi, M. H. Yi, B.-H. Ryu, *J. Mater. Chem.,* 2011, **21**, 10619-10622.

5 S. Jeong, H. C. Song, W. W. Lee, S. S. Lee, Y. Choi, W. Son, E. D. Kim, C. H. Paik, S. H. Oh, B.-H. Ryu, *Langmuir,* 2011, **27**, 3144-3149.

6 K.-Y. Chun, Y. Oh, J. Rho, J.-H. Ahn, Y.-J. Kim, H. R. Choi, S. Baik, *Nat. Nanotechnol.,* 2010, **5**, 853-857.

7 M. Park, J. Im, M. Shin, Y. Min, J. Park, H. Cho, S. Park, M.-B. Shim, S. Jeon, D.-Y. Chung, J. Bae, J. Park, U. Jeong, K. Kim, *Nat. Nanotechnol.,* 2012, **7**, 803-809.

8 W. Qu, L. Zhang, G. Chen, *Biosens. Bioelectron.,* 2013, **42**, 430-433.

9 S.-F. Wang, F. Xie, R.-F. Hu, *Sensor Actuat. B-Chem,* 2007, **123**, 495-500.

10 S. Kim, J. Byun, S. Choi, D. Kim, T. Kim, S. Chung, Y. Hong, *Adv. Mater.,* 2014, **26**, 3094-3099.

11 J. Kim, Y. Piao, N. Lee, Y. I. Park, I.-H. Lee, J.-H. Lee, S. R. Paik, T. Hyeon, *Adv. Mater.,* 2010, **22**, 57-60.

12 H. Wang, X. Jiao, D. Chen, *J. Phys. Chem. C,* 2008, **112**, 18793-18797.

13 Y. Chen, D.-L. Peng, D. Lin, X. Luo, *Nanotechnology,* 2007, **18**, 505703-505708.

14 C. N. Chinnasamy, B. Jeyadevan, K. Shinoda, K. Tohji, A. Narayanasamy. K. Sato, S. Hisano, *J. Appl. Phys.,* 2005, **97**, 10J309.

15 V. Tzitzios, G. Basina, M. Gjoka, V. Alexandrakis, V. Georgakilas, D. Niarchos, N. Boukos, D. Petridis, *Nanotechnology,* 2006, **17**, 3750-3755.

16 A. Sarkar, S. Kapoor, G. Yashwant, H. G. Salunke, T. Mukherjee, *J. Phys. Chem. B,* 2005, **109**, 7203-7207.

17 M. Grzelczak, J. Pérez-Juste, B. Rodríguez-González, M. Spasova, I. Barsukov, M. Farle, L. M. Liz-Marzán, *Chem. Mater.,* 2008, **20**, 5399-5405.

18 C. W. Kim. H. G. Cha, Y. H. Kim, A. P. Jadhav, E. S. Ji, D. I. Kang, Y. S. Kang, *J. Phys. Chem. C,* 2009, **113**, 5081-5086.

19 E.M.M. Ibrahim, S. Hampel, R. Kamsanipally, J. Thomas, K. Erdmann, S. Fuessel, C. Taeschner, V. O. Khavrus, T. Gemming, A. Leonhardt, B. Buechner, *Carbon,* 2013, **63**, 358-366.

20 M. S. Bazarjani, M. M. Müller, H.-J. Kleebe, Y. Jüttke, I. Voigt, M. B. Yazdi, L. Alff, R. Riedel, A. Gurlo, *ACS Appl. Mater. Interfaces,* 2014, **6**, 12270-12278.

21 S. Mourdikoudis , V. Collière , C. Amiens , P. Fau, M. L. Kahn, *Langmuir,* 2013, **29**, 13491-13501.

22 A. P. LaGrow, S. Cheong, J. Watt, B. Ingham, M. F. Toney, D. A. Jefferson, R. D. Tilley, *Adv. Mater.,* 2013, **25**, 1552-1556.

23 M. G. Panthani, V. Akhavan, B. Goodfellow, J. P. Schmidtke, L. Dunn, A. Dodabalapur, P. F. Barbara, B. A. Korgel, *J. Am. Chem. Soc.,* 2008, **130**, 16770-16777.

24 J. Tang, S. Hinds, S. O. Kelley, E. H. Sargent, *Chem. Mater.,* 2008, **20**, 6906-6910.

25 J. Gong, L.L. Wang, Y. Liu, J.H. Yang, Z.G. Zong, *J. Alloy Compd.,* 2008, **457**, 6-9.

26 Y. Mi, D. Yuan, Y. Liu, J. Zhang, Y. Xiao, *Mater. Chem. Phys.,* 2005, **89**, 359-361.

27 S.-J. Oh, Y. Jo, E. J. Lee, S. S. Lee, Y. H. Kang, H.-J. Jeon, S. Y. Cho, J.-S. Park, Y.-H. Seo, B.-H. Ryu, Y. Choi, S. Jeong, *Nanoscale,* 2015, **7**, 3997-4004.

28 Y. Jo, S.-J. Oh, S. S. Lee, Y.-H. Seo, B.-H. Ryu, J. Moon, Y. Choi, S. Jeong, *J. Mater. Chem. C,* 2014, **2**, 9746-9753.

29 S. Jeong, S. H. Lee, Y. Jo, S. S. Lee, Y.-H. Seo, B. W. Ahn, G. Kim, G.-E. Jang, J.-U. Park, B.-H. Ryu, Y. Choi, *J. Mater. Chem. C,* 2013, **1**, 2704-2710.

30 S. Jeong, H. C. Song, W. W. Lee, Y. Choi, B.-H. Ryu, *J. Appl. Phys.,* 2010, **108**, 102805.

31 A. Kamyshny, S. Magdassi, *Small,* 2014, **10**, 3515-3535

32 S. Jeong, K. Woo, D. Kim, S. Lim, J. S. Kim, H. Shin, Y. Xia, J. Moon, *Adv. Funct. Mater.,* 2008, **18**, 679-686.

33. W. D. Callister, *Maerials Science and Engineering an Introduction*, John Wiley & Sons, Inc.

34 S. Jeong, H. C. Song, W. W. Lee, Y. Choi, S. S.Lee, B.-H. Ryu, *J. Phys. Chem. C,* 2010, **114**, 22277-22283.

35 J. Yeo, G. Kim, S. Hong, M. S. Kim, D. Kim, J. Lee, H. B. Lee, J. Kwon, Y. D. Suh, H. W. Kang, H. J. Sung, J.-H. Choi, W.-H. Hong, J. M. Ko, S.-H. Lee, S.-H. Choa, S. H. Ko, *J. Power Sources,* 2014, **246**, 562-568.

36 S. De, T. M. Higgins, P. E. Lyons, E. M. Doherty, P. N. Nirmalraj, W. J. Blau, J. J. Boland, J. N. Coleman, *ACS Nano,* 2009, **3**, 1767-1774.

Graphical Abstract

We provide the chemical methodology toward the potential for flexible, printed magnetic devices even on cost-effective polyethylene terephthalate (PET) and paper substrates, with a demonstration of an air-brush printing and an instant photonic annealing in a timescale of 10^{-3}sec.